

Adversarial Wear and Tear: Exploiting Natural Damage for Generating Physical-World Adversarial Examples

Samra Irshad, Seungkyu Lee, Nassir Navab, Hong Joo Lee, and Seong Tae Kim

arXiv:2503.21164v1 [cs.CV] 27 Mar 2025

Abstract—The presence of adversarial examples in the physical world poses significant challenges to the deployment of Deep Neural Networks (DNNs) in safety-critical applications such as autonomous driving, where even minor misclassifications can lead to catastrophic consequences. Most existing methods for crafting physical-world adversarial examples are ad-hoc and deliberately designed, relying on temporary modifications like shadows, laser beams, or stickers that are tailored to specific scenarios. In this paper, we introduce a new class of physical-world adversarial examples, *AdvWT*, which draws inspiration from the naturally occurring phenomenon of ‘wear and tear’, an inherent property of physical objects. Unlike manually crafted perturbations, ‘wear and tear’ emerges organically over time due to environmental degradation, as seen in the gradual deterioration of outdoor signboards. To achieve this, *AdvWT* follows a two-step approach. First, a GAN-based, unsupervised image-to-image translation network is employed to model these naturally occurring damages, particularly in the context of outdoor signboards. The translation network encodes the characteristics of damaged signs into a latent ‘damage style code’. In the second step, we introduce adversarial perturbations into the style code, strategically optimizing its transformation process. This manipulation subtly alters the damage style representation, guiding the network to generate adversarial images where the appearance of damages remains perceptually realistic, while simultaneously ensuring their effectiveness in misleading neural networks. Through comprehensive experiments on two traffic sign datasets, we show that *AdvWT* effectively misleads DNNs in both digital and physical domains. *AdvWT* achieves an effective attack success rate, greater robustness, and a more natural appearance compared to existing physical-world adversarial examples. Additionally, integrating *AdvWT* into training enhances a model’s generalizability to real-world damaged signs. The code for this paper will be released after review process on <https://github.com/samra-irshad/AdvWT>.

Index Terms—Adversarial examples, Image-to-image translation, Robustness.

I. INTRODUCTION

IN recent years, Deep Neural Networks (DNNs) have become increasingly popular for a wide range of computer vision tasks. Despite their success, DNNs remain vulnerable to adversarial perturbations, which significantly impact their reliability. The susceptibility of DNNs to adversarial threats poses significant concerns for their deployment in

Samra Irshad, Seungkyu Lee, and Seong Tae Kim are with School of Computing, Kyung Hee University, Gyeonggi-do 17104, South Korea (e-mail: samra@khu.ac.kr, seungkyu@khu.ac.kr, st.kim@khu.ac.kr)

Nassir Navab and Hong Joo Lee are with Technical University of Munich, Germany (e-mail: nassir.navab@tum.de, hongjoo.lee@tum.de)

Corresponding authors: Seong Tae Kim, Hong Joo Lee

safety-critical applications, such as autonomous driving and healthcare [1]–[3]. For instance, an adversary could manipulate an outdoor traffic sign in the real world, potentially causing vehicles to make dangerous decisions [4]. Recently, physical-world adversarial attacks have gained substantial attention due to the severe risks of catastrophic consequences they present [5], [6], [32].

Classified by the manner in which perturbation patterns are realized, two principal methods have emerged for crafting adversarial examples in the physical world. The first involves introducing perturbations via optical patterns, such as laser beams [5], shadows [6], or projected light [7]. The second approach entails directly altering the target object, by applying meticulously crafted adversarial patches [8], [9] or synthetic styles [13]. While these approaches have demonstrated effective attack performance, their generation relies on specific conditions. Optical pattern-based methods, for instance, may require controlled environmental factors such as a minimum brightness threshold [6] or low-light surroundings [5]. Conversely, adversarial patches are typically designed without prioritizing stealth, making them conspicuous [8].

Additionally, to maintain robustness in real-world settings, larger perturbations are injected that can endure fluctuating environmental conditions. However, this compromises stealthiness, which results in an unnatural appearance of adversarial images. Moreover, most of the existing physical-world adversarial perturbations are crafted with a single specific pattern (e.g., shadows [6], patches [9]). Utilizing a uniform pattern enables defense mechanisms to identify the distribution of adversarial patterns, facilitating effective countermeasures against such attacks [10] [30] [12].

Building on the observation that objects in outdoor environments are subject to natural degradation over time, which can alter their appearance and potentially mislead DNNs, we introduce **Adversarial Wear and Tear** (*AdvWT*), a new class of physical adversarial examples. Specifically, we focus on outdoor signs, simulating their gradual deterioration as they are exposed to environmental conditions. These perturbations result from real-world factors such as weathering, fading, corrosion, dirt accumulation, and structural wear. Unlike existing attacks, *AdvWT* perturbations emerge passively over time, making them both persistent and more difficult to mitigate. Fig. 1 compares real-world damaged signs with *AdvWT*-generated adversarial examples, demonstrating how our proposed damage simulation seamlessly integrates realistic degradation patterns.

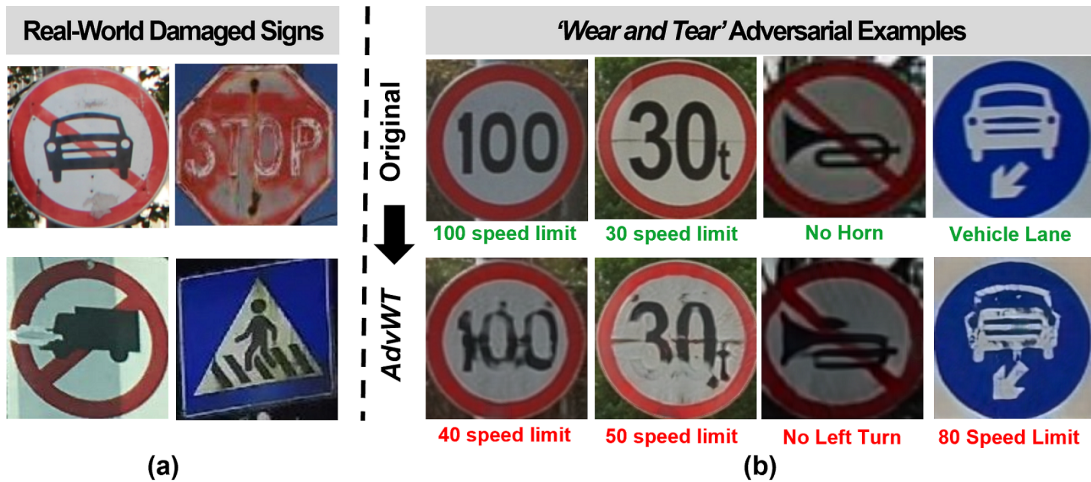


Fig. 1. Adversarial Wear & Tear Examples. (a) Damaged traffic signs observed in real-world environments. (b) Original traffic Signs (first row) with *correct predictions* and *adversarially* damaged traffic signs generated by *AdvWT* (second row) with *misclassified labels*. Our proposed adversarial perturbations not only resemble real-world degradation but also successfully manipulate model predictions.

Our perturbations introduce a new paradigm by leveraging real-world degradation as a stealthy adversarial cue. Unlike existing physical adversarial examples that can be reversed by removing the applied perturbation, *AdvWT* introduces modifications that are difficult to eliminate without physically restoring or replacing the object. Since natural damage evolves over time due to environmental exposure, these perturbations cannot be generated instantly like laser or shadow-based attacks. To address this, we simulate the physical damage using a learned damage representation. Specifically, we frame this as a damage representation learning problem and model the degradation patterns (e.g., scratches, fading, and cracks). Using an unsupervised GAN-based framework [24], we learn and optimize a latent damage representation to introduce adversarial perturbations that mislead DNNs while maintaining visual realism.

Based on the characteristics of our proposed adversarial examples, we identify four key properties for comparison: **Gradual Evolution, Occurrence Rate, Pattern Diversity, and Persistency** (Fig. 2). **Gradual Evolution** refers to damage accumulating progressively over time due to environmental exposure, in contrast to the instantaneous effects produced by light or projection-based attacks. **Occurrence Rate** refers to how frequently a perturbation appears in real-world settings where naturally damaged signs are far more common than laser or shadow-based attacks. **Pattern Diversity** captures the range of visual variations, as wear-and-tear can manifest in many forms such as cracks, fading, and discoloration. **Persistency** indicates the lasting nature of perturbations; physical degradation remains until the object is repaired, whereas others like light or shadow disappear instantly when the external stimulus is removed.

The major contributions of our paper are summarized as follows:

- We propose *AdvWT*, which leverages the ‘wear and tear’ properties of physical objects (specifically traffic signs) to craft stealthy adversarial examples. *AdvWT* generates

natural-looking adversarially damaged traffic signs, and the injected perturbation manifests in diverse patterns like cracks, corrosion, paint peeling, dirt accumulation, etc.

- Since ‘wear-and-tear’ on traffic signs develops gradually, unlike laser or shadow-based attacks, it cannot be directly applied. To address this, we introduce a framework for simulating naturally damaged traffic signs, a previously unexplored task. Unlike instantaneous perturbations, real-world degradation is stochastic and builds progressively. Our approach captures these complexities to simulate the naturally damaged traffic signs and evaluate the impact of *adversarial damage* on recognition models.
- Our approach for damage simulation utilizes a GAN-based unsupervised Image-to-Image (I2I) translation framework [24] to learn the style representations of damaged traffic signs. Subsequently, we explore the latent space to identify adversarially damaged codes, enabling a controlled generation of realistically degraded signs.
- Through extensive experiments, we verify that the proposed *AdvWT* successfully fools DNNs in digital and physical domains. The adversarial perturbations generated by *AdvWT* demonstrate better adversarial robustness and naturalness. Furthermore, training with *AdvWT* can improve generalizability against real-world damaged outdoor signs.

II. RELATED WORK

A. Adversarial Examples

First introduced by [14], adversarial examples are subtle and imperceptible perturbations that can cause deep neural networks (DNNs) to misclassify when added to an input. Since their discovery, the robustness of DNNs against various adversarial threats has been extensively studied [15], [17], [18], [43]. These threats manifest in both digital and physical domains. In digital domain, adversarial examples are typically generated by constraining the perturbation magnitude using norms such as the l_∞ -norm [19], l_2 -norm, and l_0 -norm [15], ensuring their imperceptibility. In contrast, adversarial examples designed

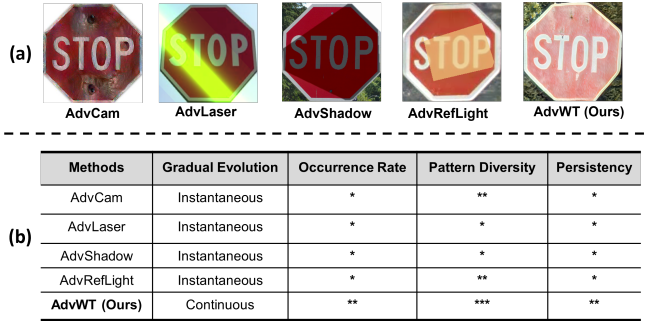


Fig. 2. Comparison of physical-world adversarial examples: (a) Examples of AdvCam [13], AdvLaser [5], AdvShadow [6], AdvRefLight [32], and AdvWT (ours). (b) Methods are compared in terms of gradual evolution, occurrence rate, pattern diversity, and persistency. Asterisks indicate presence: * (low), ** (moderate), *** (high)

for physical-world scenarios are often more conspicuous and unrestricted, as they must withstand the transformation from the physical scene to the digital input [44]. Factors such as lighting conditions, pose, and distance further attenuate the effectiveness of these perturbations [20]. Given the ubiquity of such adversarial vulnerabilities in real-world environments, numerous studies have investigated their implications. Building upon this foundation, this paper explores adversarial perturbations that leverage the natural ‘wear and tear’ properties of physical objects, a phenomenon inherently present in the physical world.

B. Physical-world Adversarial Examples

The feasibility of adversarial examples in the physical world was first demonstrated by [21]. These adversarial examples are typically designed to be printed and subsequently captured by a camera [21]. Existing methodologies generally fall into two distinct categories: contactless and contact-based adversarial examples.

1) *Contactless Physical Adversarial Examples*: Contactless adversarial examples exploit optical manipulations to perturb objects or images by altering light sources. These methods typically involve projecting laser beams [5], illuminating targets with specialized light sources [31] [7], utilizing neon beam [46] or casting shadows [6]. Duan et al. [5] introduced an attack that employs precisely optimized laser projections to mislead DNNs. Similarly, Zhong et al. [6] devised a shadow-based adversarial attack, leveraging simulated shadows to deceive DNNs. Wang et al. [32] proposed a reflected light attack, manipulating the position, geometry, and pattern of reflections to generate adversarial perturbations. Yunfei et al., [35] utilized reflection as a perturbation pattern to craft adversarial examples. Sayles et al., [45] mimicked the roller shutter effect of cameras to craft the adversarial examples. While these techniques offer a high degree of stealth, their effectiveness is inherently dependent on specific lighting and environmental conditions.

2) *Contact-based Physical Adversarial Examples*: Contact-based adversarial approaches manipulate target objects by physically attaching perturbative elements, such as stickers [8], [9], [20], scratches [47] or by directly altering their visual

appearance [13], [22]. Wei et al., [34] proposed an attack based on adversarial stickers to fool the models in physical-world. Duan et al. [13] employed neural style transfer to generate adversarial examples. However, the textures in the adversarial examples [13] sometimes appear artificial. This is due to the incomplete disentanglement of content and style representations, causing style patterns to be overly imposed on the content rather than seamlessly integrating with it. Consequently, the generated adversarial examples lack fine-grained realism, making them visually inconsistent with natural variations. Other contact-based methods have focused on perturbing image feature representations in latent space rather than directly modifying pixel values [23]. Despite their potential, these approaches often overlook semantic local structures, resulting in adversarial images that appear unrealistic and lack perceptual quality.

III. PROPOSED METHOD

A. Preliminaries

Consider a DNN-based classifier $\mathcal{F}(x) : \mathbb{R}^h \rightarrow \mathbb{R}^q$ trained to predict the label of an input image x with a ground-truth label y . Here, h represents the dimensionality of the input feature space, while q denotes the number of possible output classes. To classify x , the model produces probability scores using **softmax** function.

$$p(g|x) = \frac{e^{\phi_g(x)}}{\sum_{j=1}^q e^{\phi_j(x)}} \quad (1)$$

where $p(g|x)$ represents the probability of x belonging to class g . $\phi_g(x)$ is the model’s logit score for class g . The denominator sums over all q class logits $\phi_j(x)$, ensuring the probabilities sum to 1. The final predicted label \hat{y} is determined by selecting the class with the highest probability.

$$\hat{y} = \arg \max_{g \in 1, \dots, q} p(g|x) \quad (2)$$

The objective of an adversarial attack is to induce a misclassification such that $\arg \max_g p(g|x) \neq \arg \max_g p(g|x_{adv})$ where $g \in \{1, \dots, q\}$. The perturbation applied to generate x_{adv} must remain subtle and visually natural to human observers. In the physical world, adversarial examples are subject to additional constraints beyond visual subtlety. These perturbations are mostly inspired by or hidden within naturally occurring phenomena such as shadows or light-based projections. Therefore, effective physical-world adversarial perturbations should preserve photorealism, physical plausibility, and long-term persistence in real-world conditions.

B. Adversarial Wear and Tear Examples

Our proposed method, *AdvWT*, leverages the visual effects of physical wear and tear to craft adversarial examples. To effectively model and simulate real-world damage patterns on traffic signs, we approach this task as a **damage representation learning** problem, where the goal is to capture the underlying characteristics of both clean and damaged signs. Unlike light-based attacks that require immediate external

projection, natural damage emerges progressively due to continuous environmental exposure. We leverage a StarGAN-v2 model [27] to learn the distinct features that define different types of degradation. Within this framework, we define two stylistic domains: **(a). The damaged domain**, which encodes diverse patterns of wear and tear observed in real-world traffic signs and **(b). The clean domain**, which represents the pristine characteristics of undamaged signs. The damage style code serves as a latent representation of the degraded domain, encoding the structural and textural attributes of damaged signs. By sampling from this learned space, we can synthesize visually coherent damaged variations while ensuring that the fundamental identity of the traffic sign is preserved. This learned damage representation provides a foundation for further adversarial manipulation in the latent space.

1) *Simulating Damaged Traffic Signs*: We use StarGAN-v2 to learn a latent damage representation that realistically simulate traffic sign degradation, an unexplored area in adversarial robustness and image-to-image translation. This framework (shown in Fig. 3) consists of a **Style Encoder** $E(x)$, a **Noise-to-Style Mapping Network** $M(z)$, an image **Generator** $G(x; s)$, and a **Discriminator** D . The style representations of clean and damaged traffic signs are encoded in style vectors, denoted as s_c and s_d , respectively. The style code s is either extracted from a reference image via the style encoder $E(x)$ or generated from a randomly sampled latent vector $z \sim N(0, 1)$ mapped through $M(z)$. To integrate the style information into the generator G , Adaptive Instance Normalization (AdaIN) [25], [26] is employed. To ensure high-fidelity translations that maintain structural integrity while introducing realistic damage patterns, we incorporate a loss which is a weighted combination of seven objectives [24], [27], as shown in 3. This loss ensures that the generator not only learns the domain translation but also preserves the visual authenticity of simulated damage.

$$\lambda_1 L_{sty} + \lambda_2 L_{ds} + \lambda_3 L_{cyc} + \lambda_4 L_{adv} + \lambda_5 L_{tri} + \lambda_6 L_{kl} + \lambda_7 L_{cont} \quad (3)$$

L_{sty} is the *style reconstruction loss* [28] which ensures that the generated image $E(G(x, s))$ accurately reflects the desired wear-and-tear characteristics encoded in s , such as dirt, fading, or scratches. By aligning the generated image's style with the target damage style code, L_{sty} helps guide the generator to apply realistic and domain-consistent degradation effects.

$$L_{sty} = \mathbb{E}_{x \sim X, s \sim S} [\|s - E(G(x, s))\|_1] \quad (4)$$

L_{ds} is the *diversity sensitivity loss* [24], whereas s_1 and s_2 are style codes sampled from the same domain. This loss ensures that the generator does not collapse to a limited set of damage appearances and promotes the generation of a wide range of degradation patterns.

$$L_{ds} = -\mathbb{E}_{x \sim X_i, (s_1, s_2) \sim S_i} [\|G(x, s_1) - G(x, s_2)\|_1] \quad (5)$$

L_{cyc} is the *cyclic consistency loss* [24], that pushes the generator G to preserve the semantic identity of the input sign x to remain unchanged during translation. This is crucial for

maintaining the functional meaning of the sign while applying realistic damage patterns.

$$L_{cyc} = \mathbb{E}_{x \sim X, s \sim S} [\|x - G(G(x, s), E(x))\|_1] \quad (6)$$

L_{adv} is the *adversarial loss* [24], that predicts if the image x is a real image of its domain or fake image. We set λ_4 to 1.

$$L_{adv} = \mathbb{E}_{x \sim X_i, s \sim S_j} [\|\log D_i(x) + \log(1 - D_j(G(x, s)))\|] \quad (7)$$

L_{tri} is the *triplet loss* that enforces domain disentanglement by clustering style codes within the same domain while enforcing separation between different domains. In accordance with the standard triplet loss formulation [29], an anchor style code s_a and a positive style code s_p are both extracted from the same domain ($s_a, s_p \in S_i$), whereas the negative style code s_n is drawn from a different domain ($s_n \in S_j, j \neq i$), as shown in Fig. 3. These style representations are obtained by sampling real images and encoding them through the style encoder. The margin parameter β (set as 0.1 in our case) regulates the extent of separation between clusters in the style space, preserving the distinctiveness of domain-specific features. This loss helps the model learn domain-specific damage patterns more effectively by maintaining a well-separated and interpretable latent style space.

$$L_{tri} = \mathbb{E}_{(s_a, s_p, s_n) \sim S} [\max(\|s_a - s_p\| - \|s_a - s_n\| + \beta, 0)] \quad (8)$$

L_{kl} is the KL-divergence loss that enforces a prior Gaussian distribution on the set of all the style codes to encourage a compact space S . Enforcing this constraint allows smooth transitions between different styles of degradation and ensures that randomly sampled latent codes correspond to realistic and semantically meaningful damage patterns.

$$L_{kl} = \mathbb{E}_{s \sim S} [\|D_{KL}(p(s) || N(\mathbf{0}, \mathbf{I}))\|] \quad (9)$$

L_{cont} is the *content preservation loss* [24], that constraints the generator G to preserve the content of source image x . It ensures that while the visual appearance of traffic signs is modified to reflect realistic wear-and-tear, the core identity remains unchanged. This is crucial to avoid altering the sign's intended meaning while simulating natural degradation. We set the values of λ to 1, except for λ_1 which is set to 2.

$$L_{cont} = \mathbb{E}_{x \sim X, s \sim S} [\psi(x, G(x, s))] \quad (10)$$

2) *Damage-Aware Latent Style Optimization*: After training the image-to-image translation GAN, we obtain style vectors that capture the distinct visual characteristics of clean and damaged traffic signs, enabling bidirectional translation. The style code, an N -dimensional latent representation, encodes the transformation dynamics between these two domains. Given a clean traffic sign x_c and a damage style code s_d , the generator synthesizes a realistically degraded version x_d .

To generate our proposed *AdvWT* perturbations, we introduce an approach that iteratively manipulates learned style vectors to craft adversarial examples disguised as *natural physical damage*. Our approach exploits the style space of a trained latent damage representation model and optimizes the styles to induce misclassification. Specifically, we search for an **adversarially damage code** s_{adv} in the style space,

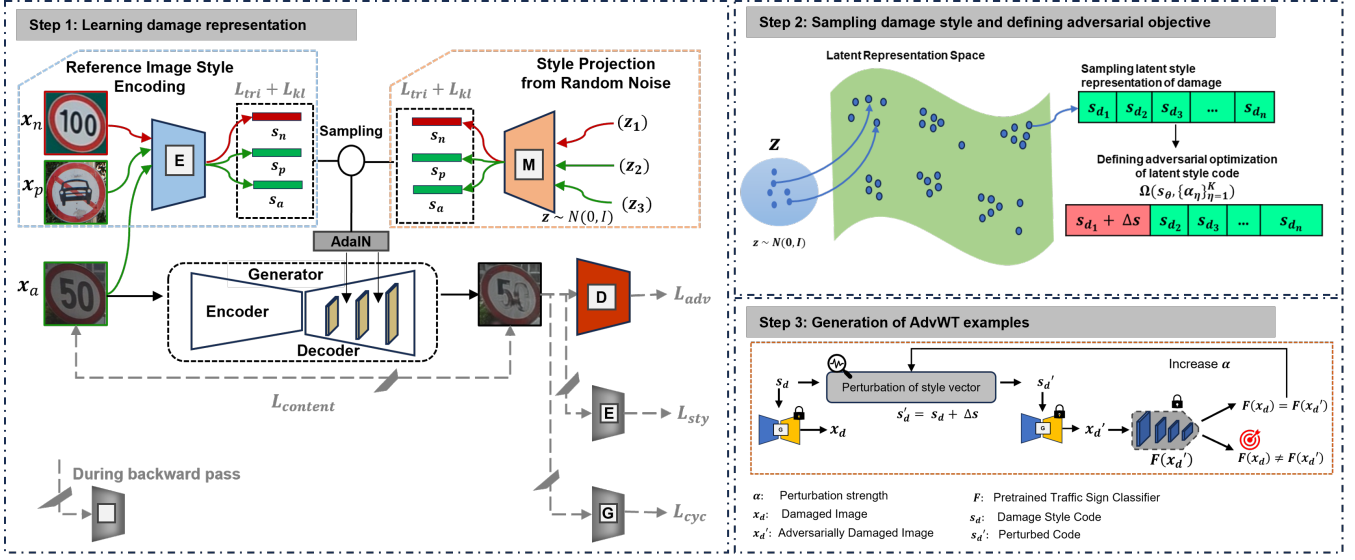


Fig. 3. Our approach for generating *AdvWT* examples. Step 1: Training phase of image-to-image translation model, which learns to represent both clean and damaged traffic signs. This framework enables the model to learn a latent representation of traffic sign degradation, capturing the natural variations in wear and tear while maintaining perceptual realism. Step 2: Generating damage styles by sampling latent noise z from a Gaussian distribution and then mapping it into a structured latent space that encodes damage styles via style projector $M(z)$. We define the adversarial style code optimization objective Ω . Step 3: Adversarial style code search algorithm iteratively applies small perturbations Δs to damage style code s_d to generate adversarial examples. Images generated by perturbing the style code are evaluated on the classifier \mathcal{F} and the perturbation strength α is increased to maximize the attack success.

such that the generator synthesizes an adversarially damaged image x_{adv} that appears visually plausible yet fools the target classifier (as illustrated in step 2 and step 3 in Fig. 3). This latent space adversarial optimization enables structured and semantic perturbations that blend seamlessly with real-world wear and tear. The details of our algorithm for finding adversarial code are provided in Algorithm 1.

We begin by sampling a random latent noise vector $z \sim \mathcal{N}(0, 1)$ and generating the initial damage style code s_d using the trained style projector $M(z)$. The style code s_d encodes damage-specific characteristics and determines the appearance of the generated image. This style code controls different aspects of the visual attributes of damage. To initialize the optimization process, we set $s_\theta = s_d$, treating s_d as the starting point for iterative refinement. Using the initial s_θ , we generate the damaged traffic sign x_d and classify it with the pre-trained model \mathcal{F} . We assume the predicted class \hat{y} corresponds to the correct class. The confidence score for \hat{y} , denoted as $p(\hat{y}|x_d)$, is recorded along with its associated style code s_θ .

We define the damage latent optimization process as Ω , which is formulated as:

$$\Omega(s_\theta, \{\alpha_\eta\}_{\eta=1}^K) = \arg \min_{s_\theta} p(\hat{y}|G(x', s_\theta + \alpha|s_\theta|)) \quad (11)$$

The goal of the optimization process Ω is to iteratively refine damage representation s_θ such that the generated image $G(x', s_\theta + \alpha|s_\theta|)$ minimizes the classifier's confidence in the correct class. Our proposed adversarial damage style optimization follows a guided stochastic search approach that balances exploration and exploitation by iteratively refining the style code s_θ . The perturbation $\alpha|s_\theta|$ modulates the style code, and controls the extent of modification in the generated damaged image. We define the search space around the initial style code s_θ where perturbations are applied proportionally to

each element's magnitude. This ensures that style components with stronger influence undergo larger perturbations while weaker components are modified more subtly. The perturbation strength α is progressively increased from c_{min} (0.1) to c_{max} (1.5) over K (15) steps. This adaptive scaling allows the search to start with small perturbations gradually explore a wider range of perturbations to maximize attack success as α increases.

At each step η , we scale the perturbation strength α and compute perturbation offsets Δs for each element of s_θ . We then establish a bounded search region $[s_\theta^-, s_\theta^+]$ corresponding to the applied perturbation α . Following Monte Carlo Sampling approach, we randomly sample a batch of T (30) candidate style codes within the dynamically updated perturbation bounds $[s_\theta^-, s_\theta^+]$. This allows the optimization to explore diverse perturbations while respecting constraints. Each candidate style code is used to generate an adversarial image $G(x', s_\theta + \alpha|s_\theta|)$, which is then evaluated on the classifier. The perturbation that minimally preserves confidence in the correct class is selected, and the process is iteratively refined toward a stronger adversarial transformation.

If none of the style vectors in the current population induces an adversarial misclassification, the perturbation factor α is incrementally increased within its allowable range. The search space is then recomputed, updating the perturbation bounds, followed by the generation of a new population of style vectors. This process is repeated iteratively until an adversarial style code is identified or the perturbation factor reaches its predefined maximum threshold.

IV. EXPERIMENTS

In this section, we introduce the datasets used in our study and experimental evaluations to assess the effectiveness of our

Algorithm 1 Pseudocode for finding adversarial damage style code

INPUT: Clean input x ; Trained style projector $M(z)$; Random Noise z ; Perturbation range $[c_{\min}, c_{\max}]$; Step size η ; Number of style vectors sampled for each step T ; Target traffic sign classifier \mathcal{F}

OUTPUT: Adversarial damage style code s_{adv}

```

1:  $z \sim N(0, 1)$ 
2: Initialize  $s_{\theta} \leftarrow M(z)$ 
3: Generate damaged traffic sign  $x_d \leftarrow G(x; s_{\theta})$ 
4: Predict the class label  $\hat{y} = \arg \max_g p(g|x_d)$ 
5: Set  $\text{Conf}_{\theta} \leftarrow p(\hat{y}|x_d)$ 
6: Set  $s_{\text{best}} \leftarrow s_{\theta}$ 
7: for  $\alpha \leftarrow c_{\min}$  to  $c_{\max}$  with step  $\eta$  do
8:   Compute perturbation:  $\Delta s_{\theta} \leftarrow \alpha |s_{\theta}|$ 
9:   Define bounds:  $s_{\theta}^+ \leftarrow s_{\theta} + \Delta s_{\theta}$ ,  $s_{\theta}^- \leftarrow s_{\theta} - \Delta s_{\theta}$ 
10:  // Generate and evaluate  $T$  images
11:  From  $[s_{\theta}^-, s_{\theta}^+]$  range, sample  $T$  style vectors
12:  Generate images:  $\{x'_i\}_{i=1}^T \leftarrow \{G(x; s_{\theta_i})\}_{i=1}^T$ 
13:  Compute classifier scores:  $\{p_i\}_{i=1}^T \leftarrow \{\mathcal{F}(x'_i)\}_{i=1}^T$ 
14:  // Check for adversarial success
15:  for  $i = 1$  to  $T$  do
16:    if  $\arg \max p_i \neq \arg \max p(x_d)$  then
17:      Return  $s_{\text{adv}} = s_{\theta_i}$ 
18:    else if  $p_i < \text{Conf}_{\theta}$  then
19:      // Track most adversarial-like style vector
20:       $\text{Conf}_{\theta} \leftarrow p_i$ 
21:       $s_{\text{best}} \leftarrow s_{\theta_i}$ 
22:    end if
23:  end for
24:  if No adversarial style code found then
25:     $s_{\theta} \leftarrow s_{\text{best}}$  // Update style vector for next iteration
26:    Increase perturbation factor:  $\alpha \leftarrow \alpha + \eta$ 
27:    Expand search bounds:  $\Delta s_{\theta} \leftarrow \alpha |s_{\theta}|$ 
28:    do Repeat search with updated parameters
29:  end if
30: end for

```

proposed adversarial attack, *AdvWT*. Our evaluation framework examines *AdvWT* across multiple dimensions, including evaluation in both digital and physical settings, perceptual naturalness, adversarial robustness, stability of perturbations under weather changes and out-of-distribution generalizability.

A. Datasets

The dataset we use consists of 4,529 traffic sign images, comprising 2,272 damaged and 2,257 undamaged signs. These images were sourced from various online repositories and publicly available traffic sign benchmarks (TSRD¹, Kaggle², DFG³ [36], CVL⁴ [37], and TTcent⁵ [38]). This dataset is used to train the image-to-image translation network. To assess the effectiveness of our adversarial examples, *AdvWT*, we use two traffic sign datasets as described below:

¹<http://www.nlpr.ia.ac.cn/pal/trafficdata/recognition.html>

²<https://www.kaggle.com/datasets/andrewmvd/road-sign-detection>

³<https://www.vicos.si/resources/dfg/>

⁴<https://www.cvl.isy.liu.se/research/datasets/traffic-signs-dataset/>

⁵<https://cg.cs.tsinghua.edu.cn/traffic-sign/>

TABLE I
ATTACK SUCCESS RATE (%) OF *AdvWT* ACROSS DIFFERENT MODELS ON HYBRID AND GTSRB-HQ DATASETS

Dataset	ResNet-18	ResNet-50	Vit-32
Hybrid	96.20	85.76	86.30
GTSRB-HQ	99.68	92.21	83.80

- **Hybrid Dataset:** This dataset comprises 2,199 training images and 604 test images, spanning 14 road sign classes.
- **GTSRB-HQ Dataset:** Constructed by filtering high-quality images from the GTSRB traffic dataset, it contains 1,504 training images and 309 test images, covering 10 road sign classes.

B. Implementation Details

We quantitatively assess the effectiveness of *AdvWT* by evaluating its impact on three trained traffic sign recognition models (ResNet-18, ResNet-50 and Vit-32). These models are trained separately on each of the aforementioned datasets. We evaluate the attack effectiveness of our proposed method, *AdvWT*, using Attack Success Rate (ASR). ASR denotes the fraction of images that are attacked successfully among the total number of test images, and a higher score shows a strong attack ability.

C. Attack Effectiveness

Table I presents the attack effectiveness in terms of ASR. *AdvWT* consistently achieves a high ASR across different datasets and models. We attribute this strong performance to its ability to simulate naturalistic damage patterns that closely resemble real-world wear and tear, rather than relying on artificial overlays or externally projected perturbations. By embedding adversarial cues within realistic degradation, *AdvWT* creates perturbations that blend seamlessly into the image, making them harder to detect and more robust in practice.

D. Ablation Study of Perturbation Strength α

AdvWT, introduces a novel mechanism to control the severity of generated damage by adjusting the magnitude of perturbation (α) applied to the damage style code. By increasing α , we can generate highly damaged adversarial examples with stronger attack effectiveness. Conversely, limiting the perturbation range preserves the natural appearance of the image but reduces the ASR. This phenomenon reveals an inherent trade-off between naturalness and adversarial effectiveness, where increasing perturbation enhances attack strength at the cost of perceptual realism.

To systematically analyze this trade-off, we conduct an ablation study, evaluating the impact of varying perturbation magnitude on both ASR and naturalness. We measure image similarity using Structural Similarity Index (SSIM) [33] to quantify how closely the adversarially generated images resemble their original counterparts. The results, presented in

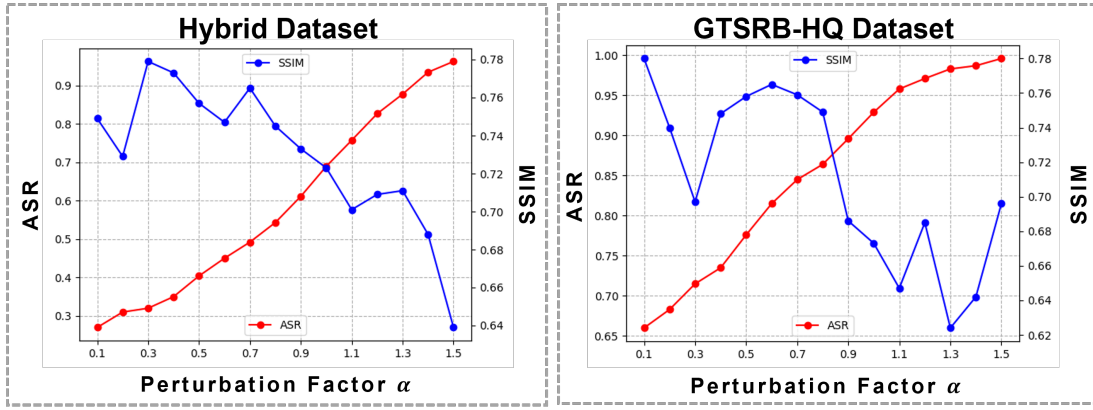


Fig. 4. Trade-off between adversarial strength and perceptual similarity: As the perturbation factor α increases, Attack Success Rate (ASR) improves (red line), while structural similarity (SSIM) with the clean image decreases (blue line). This illustrates the inherent balance between damage severity and visual realism in *AdvWT*.

Fig. 4, demonstrate that ASR (red line) increases as the perturbation range expands, whereas SSIM (blue line) decreases, indicating greater perceptual deviation from the clean image. This aligns with our hypothesis that severely damaged traffic signs exhibit lower similarity to their undamaged versions due to the intensity of projected degradation.

E. Qualitative Results

As illustrated in Fig. 5, *AdvWT* generates natural-looking damaged traffic signs that closely resemble real-world wear and tear, making the simulated damage visually indistinguishable from actual deterioration. In comparison, *AdvLaser* [5] introduces high-intensity laser patterns that appear less natural due to their pronounced brightness. In certain instances (e.g., first row), the laser effect may partially obscure the sign, drawing visual attention. *AdvShadow* [6], on the other hand, introduces shadow-based perturbations that provide meaningful occlusion; however, some of the generated shadows exhibit simplified geometries. While these shadows are effective for attack purposes, they may differ from the irregular and diffuse patterns commonly observed in real-world scenarios. *AdvCam* [13] introduces natural texture perturbations, that are visually subtle, but may still be distinguishable under close inspection. *AdvRefLight* [32] applies adversarial reflection-based perturbations, typically manifesting as localized color flashes or highlights. Although effective at misdirection, these reflections can occasionally resemble lighting artifacts that are less commonly seen in structured sign surfaces.

F. Human Study for Naturalness Evaluation

To evaluate the perceptual realism of our proposed method, we conducted a human subjective study with 32 participants to assess the naturalness of generated images. We select *AdvLaser* [5] and *AdvShadow* [6] as representative methods for comparison. Each participant was presented with a diverse set of images, including real traffic signs and adversarial examples from *AdvLaser* [5], *AdvShadow* [6], and our method *AdvWT*. For each method, we generated 10 images, and participants were asked to rate their naturalness on a 5-point Likert scale

TABLE II
NATURALNESS SCORE COMPARISON RESULTS WITH OTHER METHODS.
THE CLOSER THE SCORE IS TO 5, THE MORE NATURAL IT IS.

Method	Naturalness
Real Image	4.17
<i>AdvLaser</i> [5]	2.17
<i>AdvShadow</i> [6]	1.66
<i>AdvWT</i> (Ours)	3.66

(1 = highly unrealistic, 5 = highly realistic). The results, summarized in Table II, reveal that *AdvWT* consistently achieved higher naturalness scores, closely aligning with the perceived realism of actual traffic signs. This demonstrates the effectiveness of our approach in producing plausible damage effects, further distinguishing it from existing adversarial methods that introduce unnatural or visually conspicuous artifacts.

G. Physical Domain Experiments

To assess the real-world applicability, we perform experiments to determine whether *AdvWT* perturbations remain effective beyond the digital domain. We assess the effectiveness of *AdvWT* in both indoor and outdoor settings, capturing the influence of varying lighting and environmental conditions. Specifically, we attack ‘50 speed limit’ sign and print both clean and adversarial versions using an EPSON L8180 printer. These printed signs are then photographed using an iPhone 11 from different distances and angles, mimicking real-world viewing conditions. The captured images are subsequently analyzed by a trained traffic sign classifier.

The results of our physical-world experiments are illustrated in Figure 6. Each image is labeled with its predicted class and the classifier’s confidence score. As shown, *AdvWT* generates realistic degradations which are sufficient to mislead the classifier in varying physical conditions such as different distances and viewpoints. Furthermore, *AdvWT* adversarial examples remain potent even after undergoing real-world transformations like printing and recapturing.



Fig. 5. Visualization of adversarial examples generated by *AdvWT* and other methods: **AdvWT** can generate more diverse and realistic adversarial examples since the perturbation is embedded into the sign board through natural evolving process instead of being crafted by interaction of external projection or light.

V. FURTHER ANALYSIS

A. Adversarial Robustness

Improving adversarial robustness remains a critical challenge, with Adversarial Training (AT) [39] being one of the most effective defenses. AT enhances model resilience by incorporating adversarial examples into the training process, allowing the model to learn robust feature representations. To evaluate whether *AdvWT*-generated adversarial examples can be mitigated by AT, we implement adversarial training using *AdvWT* perturbations. Specifically, during training, we randomly apply *AdvWT* adversarial modifications to 50% of the training set images and introduce perturbations within a randomly selected range. Unlike conventional adversarial training that seeks the worst-case perturbation for each sample, we augment the training set with the perturbed images generated via randomly selected perturbation strengths that reflect the diverse and naturalistic damage variations modeled by *AdvWT*. We retrain the classifiers using this strategy and denote the resulting robust models as Hybrid_{rob} and GTSRB-HQ_{rob} , trained on Hybrid and GTSRB-HQ dataset, respectively. Table III presents a comparative analysis of model robustness. We define **benign accuracy** as the model's classification performance on clean images, while **AdvWT-AT** refers to the classification accuracy achieved with adversarial training. Additionally, we report the average number of queries required for a successful attack. Adversarial training significantly reduces model vulnerability to *AdvWT*-based attacks, yet even with adversarial training, the attack success rate remains around 50% on the Hybrid dataset, underscoring the strength of *AdvWT* perturbations. Furthermore, adversarially trained models demonstrate improved recognition performance on clean test images, suggesting that *AdvWT*-generated adversarial examples may serve as an effective augmentation strategy for improving real-world robustness. We also note that

TABLE III
EVALUATION OF ADVERSARIAL ROBUSTNESS WITH AND WITHOUT ADVERSARIAL TRAINING USING *AdvWT* EXAMPLES.

Method	Accuracy (%)	
	Benign	<i>AdvWT-AT</i> (Queries)
Hybrid	96.5	4.6 (166.57)
Hybrid_{rob}	98.0	50.7 (377.37)
GTSRB-HQ	99.6	1.3 (31.53)
GTSRB-HQ_{rob}	99.6	36.4 (388.53)

TABLE IV
OUT-OF-DISTRIBUTION GENERALIZATION ON REAL-WORLD DAMAGED TRAFFIC SIGNS

Model	Accuracy (%)
Baseline	90.1
Baseline+Corrupt	93.4
Baseline+ <i>AdvWT</i>	95.4

the number of queries required to fool the model increases in case of adversarial trained model *AdvWT-AT*.

B. Out-of-Distribution Generalization

Real-world damaged traffic signs pose a significant challenge to DNNs, leading to potential failures in safety-critical applications. To investigate whether training with *AdvWT*-generated adversarial damage patterns enhances out-of-distribution (OOD) generalization, we conduct an experiment on real-world damaged traffic signs. We compare the generalization performance of three models:

- 1) **Baseline:** Trained without augmentation.
- 2) **Baseline + Corrupt:** Trained with simulated common visual corruptions [40], where each corruption type has five levels of severity. We introduce corruptions randomly per image, selecting both the corruption type and severity level.

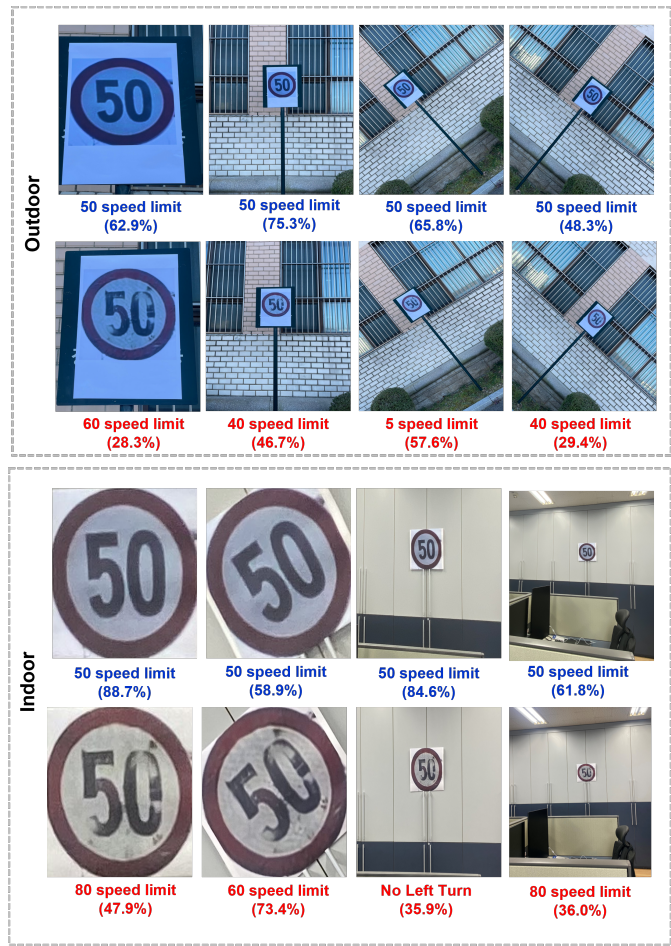


Fig. 6. Physical-world evaluation of *AdvWT* perturbation: We attack ‘50 speed limit’ sign and evaluate in indoor and outdoor environments. We show clean sign and corresponding adversarial sign. Each sign is shown with the predicted label and its corresponding confidence score. Correct predictions are shown in blue, while incorrect predictions are indicated in red. *AdvWT* can generate perturbations that are effective beyond the digital world across different environments, viewpoints, and distances.

3) **Baseline + *AdvWT*:** Trained using *AdvWT*-generated damaged signs as augmentation.

For both common corruptions and *AdvWT* augmentations, we apply perturbations with 50% probability to ensure a balanced training distribution. The results, presented in Table IV, reveal that training with *AdvWT*-generated damaged images significantly improves the model’s generalization ability to real-world damaged traffic signs compared to both the baseline and traditional corruption-based augmentation methods. This suggests that adversarially generated, semantically meaningful damage patterns offer a more effective way to enhance robustness to real-world degradation, as opposed to generic visual corruptions.

C. Interpreting Predictions of Model

We use Grad-CAM and Guided Grad-CAM to visualize the classifier’s attention and understand how different attacks influence its decision-making [41]. As shown in Fig. 7, the classifier correctly predicts the benign ‘80 speed limit’ traffic

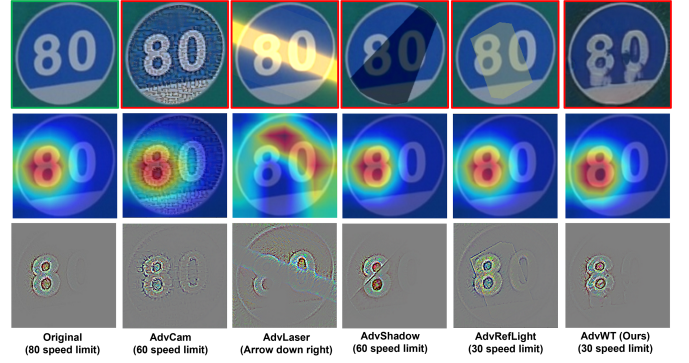


Fig. 7. Interpretability analysis using Grad-CAM and Guided Grad-CAM: Visualizing how different adversarial attacks influence the predictions of road sign classifier. The figure shows how each attack shifts or preserves the model’s attention, revealing differences in feature attribution and adversarial behavior.



Fig. 8. Visual examples showing the persistence of *AdvWT* under common environmental corruptions (brightness, blur, fog, snow) for **80** and **100** speed limit signs. Despite the distortions, the adversarial misclassification is retained, demonstrating the robustness of our perturbations in real-world conditions.



Fig. 9. Traffic sign restoration using ‘Clean Style Code’: Reversing real-World damage

sign, and attention is focused on the center of the digit ‘8’. **AdvCam** [13] shows minimal change in Grad-CAM, but Guided Grad-CAM activates over both ‘8’ and ‘0’, implying subtle distraction due to high-frequency patterns. In the **AdvLaser** attack [5], attention shifts to unrelated regions, suggesting that the high-intensity laser introduces strong distortions. **AdvShadow** [6] retains focus on relevant features but introduces misleading cues at shadow boundaries in Guided Grad-CAM visualization. **AdvRefLight** [32] preserves spatial attention in Grad-CAM, but Guided Grad-CAM highlights the edges of reflected light, indicating interference from synthetic illumination. In contrast, our proposed *AdvWT* perturbations maintain attention around semantically important regions while still achieving misclassification.

D. Stability across Weather and Visual Transformations

To evaluate the real-world applicability of our adversarial perturbations, we assess their persistence under common environmental corruptions, such as brightness shifts, blur, fog, and snow. These transformations simulate realistic conditions encountered in outdoor environments and serve as a robustness test for *AdvWT*. We apply the aforementioned distortions [40] and evaluate their effect on a pretrained traffic sign classifier. In Fig. 8, we present visual results for the **80** and **100** speed limit signs. Our findings show that *AdvWT* perturbations exhibit resilience. The classifier continues to misclassify the corrupted images, and the adversarial label is consistently preserved. While the confidence scores may slightly drift under different corruption types (e.g., decreasing from 20% to 14% after fog is added), the core adversarial behavior remains unaffected. This demonstrates that the perturbations introduced by *AdvWT* are not only effective in clean conditions but also persist under environmental distortions.

E. Application to Traffic Sign Restoration

Since our GAN model learns bidirectional mappings between undamaged and damaged domains, we explore its potential for traffic sign restoration by assessing whether it can effectively remove damage from naturally degraded images. By sampling a style code from the undamaged domain and applying it to real-world damaged traffic signs, we generate restored versions that resemble their original, undamaged state. As shown in Figure 9, our image-to-image translation model successfully reconstructs clean traffic signs from naturally damaged ones, demonstrating its ability to reverse real-world wear and tear. This suggests that beyond adversarial applications, our model has practical implications for traffic sign restoration, offering a potential solution for automated maintenance and visual enhancement of degraded road signs.

F. Discussion and Future Work

The Adversarial Wear and Tear (*AdvWT*) attack introduces a novel class of physical adversarial perturbations that mimic real-world degradation patterns such as fading, corrosion, and scratches to deceive DNNs. Unlike traditional digital perturbations or synthetic overlays, these adversarial modifications are persistent in the environment. This research highlights a previously unaddressed vulnerability in AI-driven perception systems, particularly in autonomous driving. While this work sheds light on the robustness gaps in real-world DNN deployments, it also raises important ethical considerations. The persistence of wear and tear adversarial perturbations poses a unique security challenge that differs from transient or reversible attacks. Addressing such vulnerabilities is crucial for the trustworthiness of AI systems in real-world environments. Future research must focus on developing countermeasures that can effectively distinguish between natural and adversarial wear patterns, ensuring that AI-powered systems remain resilient against long-term adversarial threats.

Future Direction: While this work focuses on adversarially damaged traffic signs, real-world physical degradation

manifests in diverse forms across different objects. For example, smartphones may suffer screen fractures, and printed documents may fade over time. Future research will explore methods to simulate adversarial degradation across various real-world objects, further expanding the understanding of naturally occurring adversarial vulnerabilities and their impact on deep learning systems.

VI. CONCLUSION

In this work, we introduce *AdvWT*, the first approach to simulate real-world physical damage on traffic signs for generating adversarial examples. Unlike conventional physical-world adversarial examples that rely on ad-hoc perturbations, *AdvWT* leverages the natural ‘wear and tear’ process as an adversarial pattern. Due to the ‘continuous evolving’ characteristic of the physical damage, we formulate the problem of ‘damaged traffic sign generation’ as a ‘damage representation learning’ problem. We successfully simulate the realistic damages on the traffic signs by leveraging unsupervised GAN-based image-to-image translation model and demonstrate that structured physical degradation can effectively fool DNNs. Our experiments in both digital and physical settings confirm the attack effectiveness, stealthiness and robustness of *AdvWT*, highlighting its potential as a realistic and naturally occurring adversarial threat. Additionally, we demonstrate that training with *AdvWT*-augmented data enhances a model’s generalizability to real-world damaged traffic signs, presenting a novel avenue for improving robustness in safety-critical applications.

REFERENCES

- [1] Mariusz Bojarski, Davide Del Testa, Daniel Dworakowski, Bernhard Firner, Beat Flepp, Prasoon Goyal, Lawrence D. Jackel, Mathew Monfort, Urs Muller, Jiakai Zhang, Xin Zhang, Jake Zhao, and Karol Zieba. End to end learning for self-driving cars, 2016.
- [2] Changhong Fu, Kunhan Lu, Guangze Zheng, Junjie Ye, Ziang Cao, Bowen Li, and Geng Lu. Siamese object tracking for unmanned aerial vehicle: A review and comprehensive analysis, 2022.
- [3] Volodymyr Mnih, Koray Kavukcuoglu, David Silver, Andrei A. Rusu, Joel Veness, Marc G. Bellemare, Alex Graves, Martin Riedmiller, Andreas K. Fidjeland, Georg Ostrovski, Stig Petersen, Charles Beattie, Amir Sadik, Ioannis Antonoglou, Helen King, Dharshan Kumaran, Daan Wierstra, Shane Legg, and Demis Hassabis. Human-level control through deep reinforcement learning. *Nature*, 518(7540):529–533, feb 2015.
- [4] Zelun Kong, Junfeng Guo, Ang Li, and Cong Liu. Physgan: Generating physical-world-resilient adversarial examples for autonomous driving, 2019.
- [5] Ranjie Duan, Xiaofeng Mao, A. K. Qin, Yuefeng Chen, Shaokai Ye, Yuan He, and Yun Yang. Adversarial laser beam: Effective physical-world attack to dnn in a blink. In *Proceedings of the IEEE/CVF Conference on Computer Vision and Pattern Recognition (CVPR)*, pages 16062–16071, June 2021.
- [6] Yiqi Zhong, Xianming Liu, Deming Zhai, Junjun Jiang, and Xiangyang Ji. Shadows can be dangerous: Stealthy and effective physical-world adversarial attack by natural phenomenon. In *Proceedings of the IEEE/CVF Conference on Computer Vision and Pattern Recognition (CVPR)*, pages 15345–15354, June 2022.
- [7] Abhiram Gnanasambandam, Alex M Sherman, and Stanley H Chan. Optical adversarial attack. In *Proceedings of the IEEE/CVF International Conference on Computer Vision*, pages 92–101, 2021.
- [8] Tom B Brown, Dandelion Mané, Aurko Roy, Martín Abadi, and Justin Gilmer. Adversarial patch. *arXiv preprint arXiv:1712.09665*, 2017.
- [9] Kevin Eykholt, Ivan Evtimov, Earlene Fernandes, Bo Li, Amir Rahmati, Chaowei Xiao, Atul Prakash, Tadayoshi Kohno, and Dawn Song. Robust physical-world attacks on deep learning visual classification. In *2018 IEEE/CVF Conference on Computer Vision and Pattern Recognition*. IEEE, jun 2018.

[10] Andrew Wang, Wyatt Mayor, Ryan Smith, Gopal Nookula, and Gregory Ditzler. Shadows aren't so dangerous after all: A fast and robust defense against shadow-based adversarial attacks. *arXiv preprint arXiv:2208.09285*, 2022.

[11] Chong Xiang, Arjun Nitin Bhagoji, Vikash Sehwag, and Prateek Mittal. Patchguard: A provably robust defense against adversarial patches via small receptive fields and masking, 2020.

[12] Pouya Samangouei, Maya Kabkab, and Rama Chellappa. Defense-gan: Protecting classifiers against adversarial attacks using generative models, 2018.

[13] Ranjie Duan, Xingjun Ma, Yisen Wang, James Bailey, A. K. Qin, and Yun Yang. Adversarial camouflage: Hiding physical-world attacks with natural styles, 2020.

[14] Christian Szegedy, Wojciech Zaremba, Ilya Sutskever, Joan Bruna, Dumitru Erhan, Ian Goodfellow, and Rob Fergus. Intriguing properties of neural networks, 2013.

[15] Nicholas Carlini and David Wagner. Towards evaluating the robustness of neural networks. In *IEEE Symposium on Security and Privacy*, 2017.

[16] Jiawei Su, Danilo Vasconcellos Vargas, and Kouichi Sakurai. One pixel attack for fooling deep neural networks. *IEEE Transactions on Evolutionary Computation*, 23(5):828–841, 2019.

[17] Yinpeng Dong, Fangzhou Liao, Tianyu Pang, Hang Su, Jun Zhu, Xiaolin Hu, and Jianguo Li. Boosting adversarial attacks with momentum. In *Proceedings of the IEEE Conference on Computer Vision and Pattern Recognition (CVPR)*, June 2018.

[18] Jiawei Su, Danilo Vasconcellos Vargas, and Kouichi Sakurai. One pixel attack for fooling deep neural networks. *IEEE Transactions on Evolutionary Computation*, 23(5):828–841, 2019.

[19] Ian J. Goodfellow, Jonathon Shlens, and Christian Szegedy. Explaining and harnessing adversarial examples, 2014.

[20] Mahmood Sharif, Srujan Bhagavatula, Lujo Bauer, and Michael K. Reiter. Accessorize to a crime. In *Proceedings of the 2016 ACM SIGSAC Conference on Computer and Communications Security*. ACM, oct 2016.

[21] Alexey Kurakin, Ian Goodfellow, and Samy Bengio. Adversarial examples in the physical world, 2016.

[22] Shengshan Hu, Xiaogeng Liu, Yechao Zhang, Minghui Li, Leo Yu Zhang, Hai Jin, and Libing Wu. Protecting facial privacy: Generating adversarial identity masks via style-robust makeup transfer, 2022.

[23] Yang Song, Rui Shu, Nate Kushman, and Stefano Ermon. Constructing unrestricted adversarial examples with generative models. *Advances in Neural Information Processing Systems*, 31, 2018.

[24] Yunjey Choi, Youngjung Uh, Jaejun Yoo, and Jung-Woo Ha. Stargan v2: Diverse image synthesis for multiple domains. *Proceedings of the IEEE Conference on Computer Vision and Pattern Recognition (CVPR)*, 2019.

[25] Xun Huang and Serge Belongie. Arbitrary style transfer in real-time with adaptive instance normalization. *Proceedings of the IEEE international conference on computer vision*, 2017.

[26] Tero Karras, Samuli Laine and Timo Aila. A Style-Based Generator Architecture for Generative Adversarial Networks. *Proceedings of the IEEE Conference on Computer Vision and Pattern Recognition (CVPR)*, 2019.

[27] Yahui Liu, Enver Sangineto, Yajing Chen, Linchao Bao, Haoxian Zhang, Nicu Sebe, Bruno Lepri, Wei Wang and Marco De Nadai. Smoothing the disentangled latent style space for unsupervised image-to-image translation. *Proceedings of the IEEE Conference on Computer Vision and Pattern Recognition (CVPR)*, 2021.

[28] Xun Huang, Ming-Yu Liu, Serge Belongie and Jan Kautz. Multimodal unsupervised image-to-image translation. *Proceedings of the European conference on computer vision (ECCV)*, 2018.

[29] Florian Schroff, Dmitry Kalenichenko and James Philbin. Facenet: A unified embedding for face recognition and clustering. *Proceedings of the IEEE Conference on Computer Vision and Pattern Recognition (CVPR)*, 2015.

[30] Chong Xiang, Arjun Nitin Bhagoji, Vikash Sehwag and Prateek Mittal. PatchGuard: A provably robust defense against adversarial patches via small receptive fields and masking. *30th USENIX Security Symposium*, 2021.

[31] Athena Sayles, Ashish Hooda, Mohit Gupta, Rahul Chatterjee, and Earlene Fernandes. Invisible perturbations: Physical adversarial examples exploiting the rolling shutter effect. *Proceedings of the IEEE Conference on Computer Vision and Pattern Recognition (CVPR)*, 2020.

[32] Donghua Wang, Wen Yao, Tingsong Jiang, Chao Li, and Xiaoqian Chen. Rfla: A stealthy reflected light adversarial attack in the physical world. *Proceedings of the IEEE/CVF International Conference on Computer Vision (ICCV)*, 2023.

[33] Zhou Wang, A.C. Bovik, H.R. Sheikh and E.P. Simoncelli. Image quality assessment: from error visibility to structural similarity world. *IEEE Transactions on Image Processing*, 2004.

[34] Xingxing Wei, Ying Guo and Jie Yu. Adversarial Sticker: A Stealthy Attack Method in the Physical World. *IEEE Transactions on Pattern Analysis and Machine Intelligence*, 2022.

[35] Yunfei Liu, Xingjun Ma, James Bailey and Feng Lu. Reflection Backdoor: A Natural Backdoor Attack on Deep Neural Networks. *European Conference on Computer Vision (ECCV)*, 2020.

[36] Domen Tabernik and Danijel Skočaj. Deep Learning for Large-Scale Traffic-Sign Detection and Recognition. *IEEE Transactions on Intelligent Transportation Systems*, 2019.

[37] Fredrik Larsson and Michael Felsberg. Using Fourier Descriptors and Spatial Models for Traffic Sign Recognition. *Scandinavian Conference on Image Analysis*, 2011.

[38] Zhe Zhu, Dun Liang, Songhai Zhang, Xiaolei Huang, Baoli Li and Shimin Hu. Traffic-Sign Detection and Classification in the Wild. *IEEE Conference on Computer Vision and Pattern Recognition (CVPR)*, 2016.

[39] Aleksander Madry, Aleksandar Makelov, Ludwig Schmidt, Dimitris Tsipras and Adrian Vladu. Towards Deep Learning Models Resistant to Adversarial Attacks. *International Conference on Learning Representations (ICLR)*, 2018.

[40] Aleksander Madry, Aleksandar Makelov, Ludwig Schmidt, Dimitris Tsipras and Adrian Vladu. Benchmarking Neural Network Robustness to Common Corruptions and Perturbations. *International Conference on Learning Representations (ICLR)*, 2019.

[41] Aleksander Madry, Aleksandar Makelov, Ludwig Schmidt, Dimitris Tsipras and Adrian Vladu. Grad-cam: Visual explanations from deep networks via gradient-based localization. *Proceedings of the IEEE international conference on computer vision (ICCV)*, 2017.

[42] Leon A. Gatys, Alexander S. Ecker and Matthias Bethge. Image style transfer using convolutional neural networks. *Proceedings of the IEEE conference on computer vision and pattern recognition (CVPR)*, 2016.

[43] Shenghong He, Ruxin Wang, Tongliang Liu, Chao Yi, Xin Jin, Renyang Liu and Wei Zhou. Type-I generative adversarial attack. *IEEE Transactions on Dependable and Secure Computing*, 2022.

[44] Ziwei Liu, Feng Lin, Zhongjie Ba, Li Lu, and Kui Ren. MagShadow: Physical Adversarial Example Attacks via Electromagnetic Injection. *IEEE Transactions on Dependable and Secure Computing*, 2025.

[45] Athena Sayles, Ashish Hooda, Mohit Gupta, Rahul Chatterjee, and Earlene Fernandes. Invisible Perturbations: Physical Adversarial Examples Exploiting the Rolling Shutter Effect. *Proceedings of the IEEE conference on computer vision and pattern recognition (CVPR)*, 2021.

[46] Chengyin Hu, Weiwen Shi, Ling Tian, and Wen Li. Adversarial Neon Beam: A light-based physical attack to DNNs. *Computer Vision and Image Understanding*, 2024.

[47] Loris Giulivi, Malhar Jere, Loris Rossi, Farinaz Koushanfar, Gabriela Ciocarlie, Briland Hitaj, and Giacomo Boracchi. Adversarial scratches: Deployable attacks to CNN classifiers. *Pattern Recognition*, 2023.